

Synthesis and characterization of organic-inorganic perovskite material for solar cell application

Himadri Sekhar Das^{a,b}, Prasanta Kumar Nandi^b, Sajal Biring^{c*} and Rajesh Das^{a*}

^aDepartment of Applied Sciences, Haldia Institute of Technology, Haldia-721 657, Purba Medinipur, West Bengal, India

^bDepartment of Chemistry, Indian Institute of Engineering Science and Technology (IIST)-Howrah, Shibpur-711 103, Botanical Garden, West Bengal, India

^cDepartment of Electronic Engineering, Organic Electronics Research Center, Ming Chi University of Technology, New Taipei City 24301, Taiwan

E-mail: rajeshhit2016@gmail.com (Corresponding Author)

E-mail: biring@mail.mcut.edu.tw (Co-Corresponding Author)

Manuscript received online 25 December 2018, accepted 19 February 2019

Organic-inorganic methylammonium lead iodide ($\text{CH}_3\text{NH}_3\text{PbI}_3$) based perovskite was prepared on mesoporous $\text{TiO}_2/\text{ZnO}:\text{Ga}$ (GZO) coated glass substrate with two step spin coating technique. Ga doped ZnO ($\text{ZnO}:\text{Ga}$) thin films have been deposited by RF-Magnetron sputtering at room temperature on glass substrate and show $4.3 \times 10^{-4} \Omega \cdot \text{cm}$ electrical resistivity alongwith high optical transmittance (above 89%) and a haze factor of 52% respectively. Mesoporous TiO_2 (mp- TiO_2) paste is coated on GZO coated glass by doctor's blending method and heat treated TiO_2 powder shows both (101) and (200) anatase phases. (101) and (200) crystalline phases are mainly responsible for higher absorption coefficient in mixed TiO_2 powder. Methylammonium lead iodide ($\text{CH}_3\text{NH}_3\text{PbI}_3$) (MAPbI_3) perovskite/ $\text{TiO}_2/\text{ZnO}:\text{Ga}$ tri-layer structure shows unique electrical and optical characteristics for organic-inorganic solar cell applications.

Keywords: $\text{CH}_3\text{NH}_3\text{PbI}_3$ perovskite, $\text{ZnO}:\text{Ga}$ thin film, optical absorption, AFM.

Introduction

Methylammonium lead iodide based perovskite ($\text{CH}_3\text{NH}_3\text{PbI}_3$) solar cells have recently made more attention due to their unique properties such as high absorption over the visible range, long diffusion length, ambipolar charge transport, high mobility and superior performance and ease of fabrication¹. Researchers are studied to improve the efficiency of the PSCs by control the surface morphology, interface engineering, crystal growth, materials and so on. Very recently, the power conversion efficiency of PSCs has been achieved more than 20%². The attractive performance of PSCs exhibit huge potential as next generation highly efficient solar cells with low cost fabrication processes³.

Indium tin oxide (ITO) and fluorine doped tin oxide ($\text{SnO}_2:\text{F}$) is currently the most widely used TCO for optoelectronic devices⁴. High cost and scare in nature of indium

makes the researchers to think about the alternative TCO materials of ITO and SnO_2 ⁵. ITO thin films has some problem such as lack of supply for mass production, cost and imperfect flexibility, basically in case of perovskite solar cell when the film bent too much conductivity is decreased and also the crack damage occurs on the surface⁶. Performance of ITO thin film degrades when in contact with the commonly used acidic (PEDOT:PSS) buffer layer^{7,8}. There is another concern that ITO is brittle that cannot stand mechanical deformation. Due to these drawbacks makes ITO is not the suitable candidate for the flexible device and perovskite solar cell. Therefore, finding substitutes to ITO film is of great significance. Doped zinc oxide ($\text{ZnO}:\text{Ga}$) thus suitable candidate for these type of application also it can be eliminate the need for ITO.

Zinc oxide can be easily doped with group III elements

such as aluminium and gallium. Some advantages of ZnO such as band gap of 3.3 eV, low toxicity, good optical and electrical properties, and chemical stability in plasma processes makes zinc oxide (ZnO) a promising alternative to commercially established ITO, SnO_2 ⁹⁻¹². Also the zinc is abundant in nature; consequently, ZnO is relatively cheap^{13,14}. Kaminski *et al.* very recently investigated on alternative transparent conductor materials including AZO and ITO¹⁵. In their study they investigated the AZO and ITO based perovskite solar cell. FTO with ITO based cell and AZO based perovskite solar cell shows the photocurrent by 4.5% and 6.5% respectively. In this experiment ZnO:Ga (GZO) based TCO was introduced. No more researchers have not reported on the doped ZnO TCO based perovskite solar cell.

Mesoporous TiO_2 (mp- TiO_2) is the most widely used electron transport material in PSCs due to its excellent physico-chemical properties, such as large band gap, chemical stability, photo-stability, non-toxicity, and low cost¹⁶. In most cases perovskite based solar cells are commonly fabricated in one step/two step spin coating¹⁷ technique for preparation of high performance device on TiO_2 /TCO/glass substrate. Here film uniformity, homogeneity and inter-connectivity are the most important issues for high performance solar cell fabrication. Most researchers commonly use commercially available ITO, SnO_2 :F based TCO films. But, mp- TiO_2 film helps not only the scaffold of the perovskite layer but also to make a smooth path for electron transport with TCO films.

No more researchers has been reported perovskite based solar cell performance deposited on doped (Al, Ga, In) ZnO films as TCO till today.

In this work, the structural, optical and electrical properties of ZnO:Ga and ZnO:Ga/ TiO_2 thin films have been studied for the application in perovskite based organic-inorganic solar cell. Role of ZnO:Ga film in the above structure have been discussed to study feasibility in comparison to the commercially available ITO, SnO_2 :F based TCO films.

Experimental

ZnO:Ga thin films were deposited on glass substrate at substrate temperature (T_s) 300 K (room temperature) by dual-target RF (13.56 MHz frequency) magnetron sputtering system (Hind High Vacuum Co. (P.) Ltd.) under non reactive environment with Argon ambient using 99.99% pure sintered

ceramic disc were used as sputtering targets (2 inch in diameter and 5 mm in thickness) and target specifications is ZnO:Ga (3 wt%). ZnO:Ga thin film is first cleaned sequentially by ultrasonication in acetone and deionized water. After cleaning the substrates were dried by the nitrogen flow. TiO_2 thin layer of thickness (20 nm) was prepared on TCO glass by Dr. Blending method. Then the films were heated to 400°C for 2 h. Organic metal based methylammonium lead iodide ($\text{CH}_3\text{NH}_3\text{PbI}_3$) perovskite was prepared on mesoporous titanium di-oxide (mp- TiO_2) coated ZnO:Ga film on glass substrate with two step spin coating technique.

PbI_2 (462 mg) was dissolved in DMF (1 ml) under magnetic stirring at 70°C for 12 h. 30 μL PbI_2 solutions were deposited on mp- TiO_2 layer by spin coating at 3000 r.p.m for 20 s. After deposition of PbI_2 the substrate were dried at 70°C for 30 min. Then the films were cooled at room temperature, 80 μL $\text{CH}_3\text{NH}_3\text{I}$ solution in 2-propanol (6 mg/mL) was sprayed on the PbI_2 films by spin coating at 400 r.p.m for 20 s and finally dried the films at 70°C for 30 min. The samples were then annealed at 90°C to ensure complete reaction between PbI_2 and $\text{CH}_3\text{NH}_3\text{I}$.

The electrical properties of both GZO and perovskite/ TiO_2 /ZnO:Ga was studied by 4-probe van-der-Pauw technique attached with Hall measurement (Ecopia-HMS-3000) set-up. Optical transmittance, absorbance and Haze data of Ga doped ZnO and the absorbance of ZnO:Ga/ TiO_2 , perovskite/ZnO:Ga/ TiO_2 thin films were measured using microprocessor controlled dual beam UV-Vis spectrophotometer (Perkin-Elmer Lambda-35). Structural characterization of TCO films was carried out by Crystallographic phase analysis X-ray diffraction (XRD) (Philips PW 1710 diffractometer) ($\text{Cu K}\alpha$, $k = 1.54178 \text{ \AA}$, 2θ scan mode). The 2D and 3D surface topography of GZO films was performed by Atomic Force Microscopy (AFM) (Multimode 8, Bruker) respectively.

Results and discussion

Electrical properties:

ZnO:Ga thin films is prepared by dual-target RF Magnetron Sputtering system on glass substrate at room temperature ($T_s = 300 \text{ K}$) using 99.99% pure sintered ceramic disc of ZnO:Ga (3 wt% Ga) sputtering target by Ar as sputtering gas, 100 Watt RF-power, 10 mbar chamber pressures. ZnO:Ga films show promising electrical properties with $\rho =$

$4.3 \times 10^{-4} \Omega \cdot \text{cm}$, $R_{\text{sh}} = 12.64 \Omega / \square$, Hall mobility ($12.0 \mu\text{-cm}^2/\text{V.s.}$) and carrier concentration ($1.2 \times 10^{21} \text{ cm}^{-3}$) with film thickness of $340 \pm 5\%$ nm and optical transmission of 89% respectively due to the high carrier density whereas the mobility is 2–3 times less compared to commercial TCO films. The electrical resistivity and Hall measurements have been carried out at room temperature on doped ZnO thin films. The carrier density and mobility of the thin films were estimated from Hall measurements. Only the mobility of the doped ZnO thin films is less than that of commercially available TCO. Poor mobility is due to either high carrier density or more amorphous region or more scattering in grain boundary region. For magnetron sputtered doped polycrystalline ZnO thin films^{18–20}, columnar growth of grains is commonly observed and hexagonal wurtzite structure are formed. During nucleation stage (i.e. for ultra-thin doped ZnO film), Zn atoms bind to the O-terminated surface, small crystallites are produced, then forms Zn-O cluster and diffuse across the surface²¹. In this way, ZnO films formation becomes complete, but less denser and stacking faults are produced that may cause for low mobility.

Optical properties:

The optical transmittance of the doped ZnO thin films with thickness of $340 \pm 5\%$ (ZnO:Ga) nm is shown in Fig. 1. The thin films of ZnO:Ga show the transmittance of 89% in the visible region of solar spectrum. The decrease of transmittance in the near infrared region results from the increase of reflectance and absorption which is attributed to the plasma

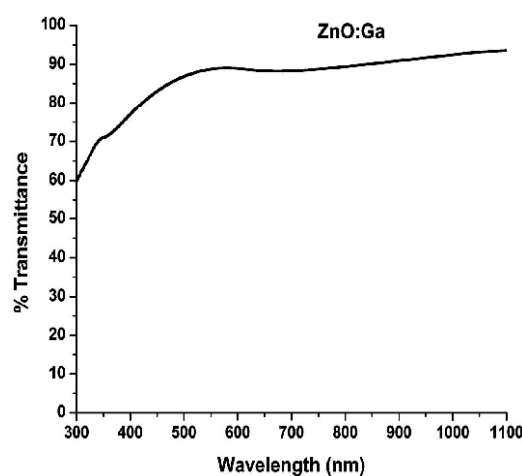


Fig. 1. Total transmittance of ZnO:Ga thin films.

resonance of the electron gas in the conduction band. The quality of the transparent conducting films can be judged by the figure of merit (ϕ) calculated from the transmittance (T) and sheet resistance (R_s) data following the equation $\phi = T^{10}/R_s^{22}$. ZnO:Ga thin films shows highest FOM of 2.4×10^{18} . The higher values of the figure of merit represent the better performance of the transparent conducting film.

GZO films shows higher transparency in visible as well as near-infrared region and a high electrical conductivity. For opto-electronics and solar cells application, both the electrical conductivity and the transmittance of TCO film should be as high as possible.

The scattering phenomenon of the films is defined by the Haze parameter²³. The Haze factor was calculated as ratio of diffuse transmittance to the total transmittance. However, for doped ZnO thin film with very rough surface, the diffuse scattering predominates which is inelastic or random. In this experiment ZnO:Ga shows 52% Haze value. Basically TCO material is used as a window layer for the incident illumination to the device and as also as serves a one of the electrodes of solar cell. The ideal TCO provides high transparency over a wide spectral range with high conductivity and higher carrier mobility.

Haze factor is defined as the ratio between the diffused transmittance and total transmission. Higher value of Haze factor means more light will be entered inside the solar cell material and ultimately effective light-trapping will be enhanced due to multiple reflections in active layer i.e. Haze factor indirectly enhances photo-response producing more number of electron hole pairs, increases the short circuit current. Finally the efficiency of the solar cell can be improved.

Haze value depends on the surface morphology of the thin films. Haze value should be high for rougher surface. This property helps the TCO to scattered more light which increases the optical absorption of weakly absorbed light in the solar cells.

The optical absorbance of are shown in Fig. 2. Fig. 2 shows the absorption spectra of perovskite $\text{CH}_3\text{NH}_3\text{PbI}_3$, $\text{TiO}_2/\text{ZnO:Ga}$ and perovskite/ $\text{TiO}_2/\text{ZnO:Ga}$ thin films.

It was clearly observed from the absorption spectra that absorption is increased after the perovskite layer deposited on the mesoporous $\text{TiO}_2/\text{ZnO:Ga}/\text{Glass}$ TCO thin film.

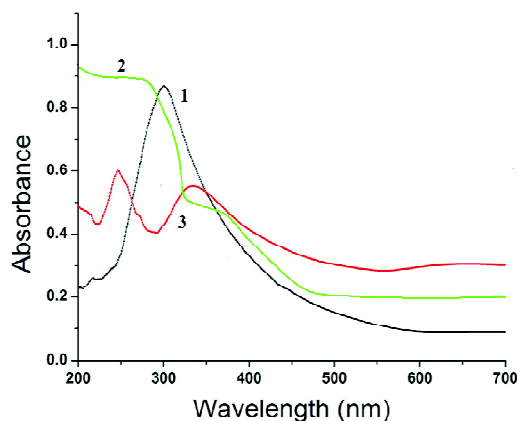


Fig. 2. Absorbance spectra of (1) perovskite $\text{CH}_3\text{NH}_3\text{PbI}_3$, (2) perovskite/ TiO_2 / ZnO:Ga , and (3) TiO_2 / ZnO:Ga coated glass.

Structural properties:

Fig. 3 shows X-ray diffraction (XRD) spectra of ZnO:Ga , ZnO:Ga/TiO_2 and ZnO:Ga/Perovskite thin films deposited at room temperature. Curve-1 shows prominent (002) peak which reveals ZnO:Ga has hexagonal-wurtzite structure with c-axis oriented crystallites perpendicular to the substrate surface. The crystallite size of TCO thin films was estimated using Scherrer's formula²⁴ and it is 5.76 nm.

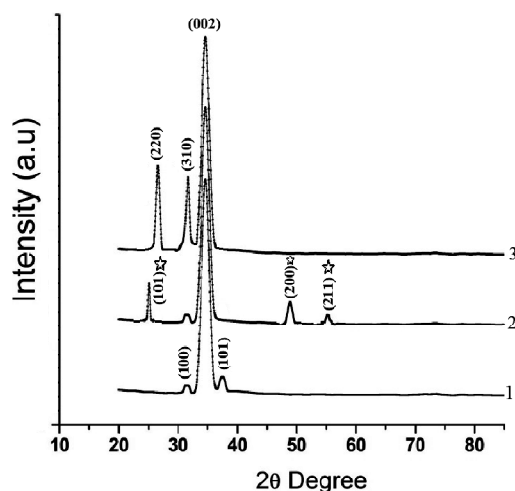


Fig. 3. X-Ray diffraction spectra of (1) glass/ ZnO:Ga , (2) glass/ ZnO:Ga/TiO_2 and (3) glass/ ZnO:Ga/perovskite thin films.

Curve-2 (Fig. 3) shows XRD spectrum of TiO_2 / ZnO:Ga bi-layer films with the diffraction peaks (101), (002), (200)

and (211) at 2θ equal to 25° , 34.33° , 49° and 55° respectively.

Average crystallite sizes are 17.01 nm as estimated from (101) phase. Here (101), (200) corresponds anatase phase and (211) is for rutile phase. Curve-3 (Fig. 3) shows (220), (310) and (002) peaks of $\text{CH}_3\text{NH}_3\text{PbI}_3/\text{ZnO:Ga}$ bi-layer samples on glass substrates with peaks position at $2\theta = 28.5^\circ$, 31.8° and 34.33° . These peaks are indicating the tetragonal perovskite structure is formed²⁵⁻²⁷ with average crystallite size 6.80 nm as estimated from (220).

Atomic Force Micrograph (Fig. 4) shows 3D topography as well as the phase of room temperature deposited ZnO:Ga films under Argon environment. 3D topography of AFM images clearly show the grain size distribution and describe the fluctuations of surface heights around an average surface height.

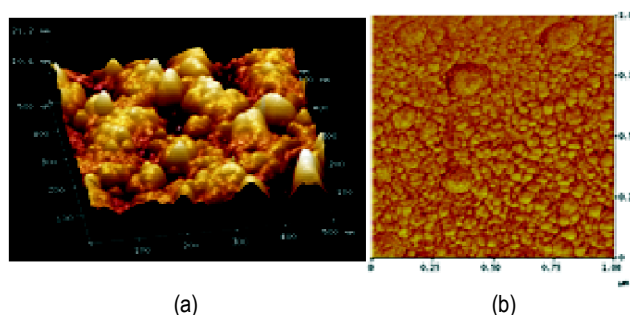


Fig. 4. AFM micrograph for (a) 3D topography of ZnO:Ga film, (b) 2D view of phase of perovskite coated ZnO:Ga thin film.

Fig. 4(b) shows the phase analysis as well as rougher and more uneven surface of perovskite coated ZnO:Ga bi-layers. This uneven surface with more numbers of grain boundary in the bi-layer film may be cause of more light absorption in perovskite layer. Sequential deposition method will leave some PbI_2 together with MAPbI_3 . A small amount of PbI_2 is helpful for decreasing the recombination providing the beneficial role. High surface coverage helps to the devices to enhance the performance devices as undesired shunting paths are minimized and as a result maximizing photo-carrier collection²⁸. Also the large surface area with large grain size crystal are in favor of more charge transport^{29,30} and increases the light scattering centers³¹ that helps to increase of effective photon absorption in active layer of

perovskite based solar cell and ultimately give rise a larger photocurrent which is one of the important advantage for its application in perovskite solar cell.

Conclusions

CH₃NH₃PbI₃ based perovskite material was deposited on ZnO:Ga/TiO₂ layer and effect of high optical transmittance (89%), stable low sheet resistance and tuneable Haze factor of ZnO:Ga thin film have been investigated. Ga doped ZnO is more stable compared to that of Al doped ZnO when subjected to moisture. Mesoporous-TiO₂ powder with (101) and (200) crystalline peaks may be responsible for strong bonding between GZO and perovskite interface. GZO creates smooth network for electron transport to perovskite material through TiO₂ interface. Granular phase of perovskite material formed on ZnO:Ga/TiO₂ layer which can indirectly influences on scattering mechanism. Crystalline phase of perovskite material is helpful for better optical absorption and that may ultimately increase the current density in perovskite based solar cell.

By changing the structure of ZnO:Ga thin film, its electrical properties will be greatly tuned to achieve higher conductivity and TiO₂ nano-powder tends to have a higher chemical stability^{5,6}. Stack of nano structured ZnO thin film⁷ and TiO₂ layer with higher dielectric constant shows less defect states, which ultimately leads to less recombination^{8,9}. Presence of (200) and (211) TiO₂ phase with (002) hexagonal wurtzite structure of ZnO:Ga play a key role to enhances of photo-response as well as maximize the device performance.

Acknowledgements

The authors highly acknowledge Department of Science and Technology & CSIR, Govt. of India for financial support [DST/TM/ SERI/2K10/67(G)] for pursuing the R&D activity.

References

1. Y. B. Bai, Q. Y. Wang, R. T. Lv, *et al.*, *Chin. Sci. Bull.*, 2016, **61**, 489.
2. H. S. Jung and N.-G. Park, *Small*, 2015, **11**, 10.
3. Y. Zhao and K. J. Zhu, *Phys. Chem. Lett.*, 2014, **5**, 4175.
4. Rakesh A. Afre, Nallin Sharma, Maheshwar Sharon and Madhuri Sharon, *Rev. Adv. Mater. Sci.*, 2018, **53**, 79.
5. N. Kim, Han-Don Um, Inwoo Choi, Ka-Hyun Kim and Kwanyong Seo, *ACS Appl. Mater. Interfaces*, 2016, **8(18)**, 11412.
6. Shudi Lu, Yang Sun, Kuankuan Ren, Kong Liu, Zhijie Wang and Shengchun Qu, *Polymers*, 2018, **10**, 5; doi:10.3390/polym10010005.
7. P. Li, C. Sun, T. Jiu, G. Wang, J. Li, X. Li and J. Fang, *ACS Appl. Mater. Interfaces*, 2014, **6**, 4074.
8. M. Jorgensen, K. Norrman, S. A. Gevorgyan, T. Tromholt, B. Andreasen and F. C. Krebs, *Adv. Mater.*, 2012, **24**, 580.
9. R. Das, H. S. Das, P. K. Nandi and S. Biring, *Applied Physics A*, 2018, **124**, 631.
10. H. S. Das, A. Dey, P. P. Roy and R. Das, *Materials Today: Proceedings*, 2017, **4**, 12610.
11. R. Das and H. S. Das, *J. Inst. Eng. India, Ser. D*, 2017, **98(2)**, 203.
12. R. Das and Himadri Sekhar Das, *J. Inst. Eng. India, Ser. D*, 2017, **98(1)**, 85.
13. E. Y. Muslih and K. H. Kim, *Materials Science and Engineering*, 2017, **214**, 012001.
14. J. Luo, J. Lin, N. Zhang, X. Guo, L. Zhang, Y. Hu, Y. Lv, Y. Zhu and X. Liu, *J. Mater. Chem. C*, 2018, **6**, 5542.
15. P. M. Kaminski, P. J. M. Isherwood, G. Womack and J. M. Walls, *Science Direct – Energy Procedia*, 2016, **2**.
16. J. Burschka *et al.*, *Nature*, 2013, **499**, 316.
17. Celline Awino, Victor Odari and Thomas Sakwa, *Coatings*, 2017, **7**, 115.
18. Jing-Chie Lin, Mao-Chia Huang, TsingHai Wang, Jian-Nan Wu, Yao-Tien Tseng and Kun-Cheng Peng, *Mater. Express*, 2015, **5(2)**.
19. S. Rahmane, M. S. Aida, M. A. Djouadi and N. Barreau, *Superlattices and Microstructures*, 2015, **79**, 148.
20. A. K. Jazmatia and B. Abdallaha, *Materials Research*, 2018, **21(3)**, e20170821.
21. J. T. Luo, A. J. Quan, Z. H. Zheng, G. X. Liang, FuLi, A. H. Zhong, H. L. Ma, X. H. Zhang and Ping Fan, *RSC Adv.*, 2018, **8**, 6063.
22. K. N. Tonny, R. Rafique, A. Sharmin, M. S. Bashar and Z. H. Mahmood, *AIP Advances*, 2018, **8**, 065307.
23. Hisham Nasser, Engin Özkol, Alban Bek and Raşit, *Turan Optical Materials Express*, 2015, **5**, 933, DOI:10.1364/OME.5.000932.
24. D. Komaraiah, E. Radha, Y. Vijayakumar, J. Sivakumar, M. V. Ramana Reddy and R. Sayanna, *Modern Research in Catalysis*, 2016, **5**, 130.
25. Qi Chen, Huanping Zhou, Ziruo Hong, Song Luo, Hsin-Sheng Duan, Hsin-Hua Wang, Yongsheng Liu, Gang Li, and Yang Yang, *J. Am. Chem. Soc.*, 2014, **136(2)**, 622; Akihiro Kojima, Kenjiro Teshima, Yasuo Shirai and Tsutomu Miyasaka, *J. Am. Chem. Soc.*, 2009, **131(17)**, 6050.
26. Shuangyong Sun, Teddy Salim, Nripan Mathews, Martial Duchamp, Chris Boothroyd, Guichuan Xing, Tze Chien

- Sum and Yeng Ming Lam, *Energy Environ. Sci.*, 2014, **7**, 399.
27. Q. Chen, H. Zhou, Z. Hong, S. Luo, H. S. Duan, H. H. Wang, Y. Liu, G. Li and Y. Yang, *J. Am. Chem. Soc.*, 2014, **136**, 622.
28. G. E. Eperon, V. M. Burlakov, P. Docampo, A. Goriely and H. Snaith, *J. Adv. Funct. Mater.*, 2014, **24**, 151.
29. I. M. Mohammed, A. A. Elbadawi and H. H. Abuellhassan, *Journal of Applied and Industrial Sciences*, 2013, **1**, 12.
30. D. Liu and Kelly, *Nat. Photonics*, 2014, **8**, 133.